CHAPTER 3

Thermodynamic Analysis of a Coal-Fired Open-Cycle MHD Power Plant

3.1 Introduction

Due to urbanization, population growth and industrialization around the globe, the world has witnessed a dramatic increase in electrical power demand in the last few decades. The conventional methods of power generation that widely depend upon fossil fuels have been reduced to some extent due to the advancement of technology and the use of non-conventional methods of energy production. Solar, wind, tidal, nuclear energy sources, etc. have been explored and harnessed to meet the demand. At the same time, all these sources and their harnessing methods could not reduce dependency on fossil fuels because of their various existing limitations compared to fossil fuel energy resources. Gas and steam turbines have been made more efficient with higher inlet temperatures due to the advancement in metallurgy and high-temperature blade and other materials. The use of conventional and most non-conventional technologies for power generation is limited by the maximum material temperature limit, wear, and tear, aging, etc. The role of Magnetohydrodynamics (MHD) as a means of power generation has been cited as one of the most potent alternatives to conventional as well as other non-conventional energy production methods because of its various advantages [1]. The MHD power system is a direct method of energy conversion that converts heat energy to electrical energy. The generator of an MHD plant is free of any rotating components, unlike power turbines. Moreover, the operating temperature for MHD can be much higher than what could be achieved by any known energy generation system. The MHD power generation concept was introduced long back, for the first time by Michael Faraday in 1832.

Faraday in his experiment found the possibility of electric power generation capacity from flowing water under the influence of the earth’s magnetic field.

Literature on MHD power reveals the continuous effort put forth by the scientific and research community, energy policymakers, and administrators around the world to establish a new, reliable, safe, and sustainable energy [1] for the current and future in the form of MHD. Various analyses and experiments were conducted to realize MHD power commercially [2, 3, 4, 8, 9, 10]. Results of MHD power and efficiency at constant velocity have shown dependency on isentropic conditions [2] when irreversibilities due to internal and external factors were considered. Processes in MHD power generation and related issues have been discussed [3], and recommended the use of other efficient subsystems. Prospects of MHD power generation depend on suitably meeting the challenges through more technological developments. In realizing MHD power, the associated demerits [4] need to be addressed and the use of MHD in existing thermal power generation plants can enhance the generation capacities [8, 9] of such plants. Recent performance analyses of the MHD power plant were based on variation in coal combustion technique [10], use of maximum power density at constant velocity for generators [11], and variation in the generator inlet both as subsonic and supersonic [12] at constant channel width. There are possibilities for temperature and velocity modulation for high power densities [13] by modulating plasma in a quasi-steady MHD combustion system. The present work analyses the performance of an MHD power plant with the variation in nozzle area ratio (i.e exit to throat area ratio of the nozzle) at a constant and subsonic nozzle inlet Mach number that has not been reported in other literature and is an alternate approach to estimating the MHD plant performance.

In the present work, a coal-fired MHD power plant is analyzed to predict its performance using a constant nozzle inlet Mach number. Two supersonic nozzles namely A and B are taken with the variation in the throat to exit area ratio. The nozzle exit parameters, adiabatic flame temperature for coal combustion, and the performance parameters of the segmented Faraday-type MHD generator are calculated using each nozzle separately. It has been found that an increase/decrease in nozzle area ratio resulted in an increase/decrease in gas velocity at the MHD generator inlet but with a reduction in temperature. The nozzle efficiency is found to be almost independent of either the area ratio or Mach number at the nozzle exit. The maximum voltage and power are found to increase with an increase in area ratio. The nozzle exit velocity and efficiencies are found to vary with the area ratio.

The present chapter reports the performance of an MHD power plant by considering the variations in nozzle area ratio at a constant and subsonic nozzle inlet Mach number and was not reported previously in the literature as to the authors' best knowledge. Results of the analyses have shown that MHD can be a potential alternative power generation technology of the future with further improvements in its efficiency and power output with related technological advancements.

3. 2 System Description

In the present work, a simple MHD power plant is considered for its performance analysis. The MHD system in this study consists of a combustor, two supersonic nozzles (analyzed separately), the MHD generator followed by a diffuser, and a seed recovery unit shown in Fig.3.1.

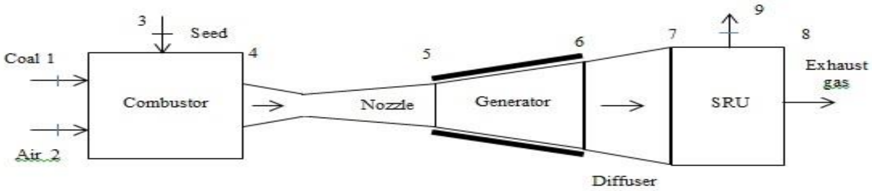

Fig. 3.1. Typical MHD power plant

The pulverized coal and preheated air are supplied to the MHD combustion chamber to which cesium (Cs) is added as a seeding material to improve the ionization and electrical conductivity of the combustion gas. The ionized gas (plasma) gets accelerated to a high velocity by passing through a converging-diverging nozzle. At high temperatures and velocity, the plasma flows through the MHD duct. The MHD duct chosen is a segmented Faraday type generator to which a strong magnetic field is applied transversely. Electric current is obtained with the use of electrodes attached to the generator walls perpendicular to the direction of conducting fluid flow and the applied magnetic field.

3.3 Thermodynamic Analysis of the MHD System

3.3.1. Fuel and air analysis

The coal for analysis has been taken as a typical Assam coal found in Karbi Anglong with the moisture and volatile matter removed and the composition within the given range and assumed data. The elemental composition (wt %) of dry-coal are C=70, H=4, O=9, S=3.4, N=1.6, A=12

The combustion reaction of coal and air is given by equation (3.1) as

$$xC + yH + zO + lS + mN + n(O_2 + 3.76N_2) \rightarrow j^*_{CO_2}CO_2 + j^*_{H_2O}H_2O + j^*_{SO_2}SO_2 + j^*_{O_2}O_2 + j^*_{N_2}N_2 \quad (3.1)$$

in equation (3.1), x, y, z, l, m are the mass fraction of coal composition, n is the stoichiometric coefficient, the asterisk j*'s* are the mole fractions of the product species. The fuel to air ratio *f*, obtained is 0.10783 using 20% excess air.

Next, the HHV of the dry coal is computed using the correlation [7] expressed by the equation (3.2) as

$$HHV = 0.3491C + 1.1783H + 0.1005S - 0.1034O - 0.0211A - 0.015N \quad (3.2)$$

The mass flow rate for coal is obtained to be 2.159 kg/s considering combustion and conversion efficiencies, heat rate, and the overall conversion efficiency, and the airflow rate is computed according to [5] expressed by the equation (3.3) as

$$\dot{m}_{air} = \frac{M_{air}}{M_{fuel}} \times \dot{m}_{fuel} \times \frac{1}{f} \tag{3.3}$$

Molecular mass for fuel and air are computed from their elemental compositions using equation (3.1). The mass flow rate of the seed material is taken as 1% of the total combined flow rates of coal and air. The flow rate of the combustion products or plasma can be obtained as

$$\dot{m}_{plasma} = \dot{m}_{air} + \dot{m}_{fuel} + \dot{m}_{seed} \tag{3.4}$$

Knowing fuel HHV and fuel flow rate, the thermal input to the MHD combustor can be obtained using equation (3.5)

$$\dot{Q}_{th} = \dot{m}_{dry\ coal} \times HHV \tag{3.5}$$

Table 3.1. Determination of mass flow rates, HHV and thermal input

Mass flow rate, $\dot{m}$, (*kg/s*)		*HHV* (*MJ/kg*)	Thermal input $\dot{Q}_{th}(MW)$
$\dot{m}_{fuel}$	2.159	28.284	61.065
$\dot{m}_{air}$	51.594		
$\dot{m}_{seed}$	0.538		
$\dot{m}_{plasma}$	54.291		

3.3.2 Estimation of adiabatic flame temperature

The adiabatic flame temperature or maximum theoretical temperature for the combustion chamber is estimated using a constant-pressure combustion process. The constant-pressure combustion tends to give a lower temperature compared to constant-volume combustion.

For a constant-pressure combustion reaction [6], the enthalpy relation of the reactants and products are given by the equations (3.6), (3.7), and (3.8) respectively as follows:

$$\sum H_{product} = \sum H_{Reactants} \tag{3.6}$$

$$\sum H_{product} = \sum_p n_k \bar{h}_{f,k}^0 + \sum_p n_k \bar{c}_{p,k}(T_{adia} - 298) \quad (3.7)$$

$$\sum H_{Reactants} = \sum_R n_i \bar{h}_{f,i}^0 \quad (3.8)$$

In equation (3.7), k is the product constituent, n_k is the number of moles of the product, T_{adia} is the adiabatic flame temperature, $\bar{c}_{p,k}$ is the mean molar specific of the product constituents, and $\bar{h}_{f,k}^0$ is the molar specific enthalpy of formation of the product *k*. In equation (3.8), i represents the reactant components, $\bar{h}_{f,i}^0$ is the molar specific enthalpy of formation of the reactant i, and n_i is the number of moles of the reactant components taking part in the combustion reaction given by equation (3.1). The mean specific heats for the constituents products, $\bar{c}_{p,k}$ are taken at an average temperature of 298 K and 4502 K (assumed adiabatic temperature) considering the ionization of the combustion products. The adiabatic flame temperature is taken at 3500 K, the value of the specific enthalpy of formation and their specific heats of the product species temperature are interpolated from the data values [6] and *JANAF Thermochemical tables* at the required temperature for the state points as shown in Fig.3.1.

3.3.3. Modeling of MHD system components

The present analysis mainly takes into account the combustor, nozzle, and the MHD generator for performance evaluation of the MHD plant that is primarily responsible for the flow of ionized gases for the generation of desired power.

3.3.3.1 MHD combustor modeling

The mass flow rates of various flow streams, thermal input, and the adiabatic flame temperature for the MHD combustor have been determined in Table 3.1 using the relations (3.2) to (3.8).

3.3.3.2. Modeling of the nozzle

The two nozzles A and B (say) in the present work differ in their area ratios. Each nozzle is assumed adiabatic and the flow through them is idealized as isentropic. The nozzle exit-flow Mach number is determined to obtain the nozzle exit temperature.

The nozzle area ratio is given by the empirical relation expressed by equation (3.9) as

$$\frac{A_e}{A^*} = (\frac{\Upsilon+1}{2})^{\frac{-(\Upsilon+1)}{2(\Upsilon-1)}} \times \frac{\left(1+\frac{\Upsilon-1}{2}M_e^2\right)^{\frac{\Upsilon+1}{2(\Upsilon-1)}}}{M_e} \tag{3.9}$$

The temperature ratio for the isentropic nozzle is given by equation (3.10) as

$$\frac{T_e}{T_{adia}} = (1 + \frac{\gamma-1}{2} {M_e}^2)^{-1}$$

(3.10)

Therefore, the velocity at the nozzle exit V_e is calculated as given by equation (3.11)

$$V_e = M_e \times c_s(T_e) \tag{3.11}$$

In equation (3.11), c_s is the sound velocity which is a function of nozzle exit temperature T_e and is expressed by the equation (3.12) as

$$c_s(T_e) = \sqrt{\gamma R T_e} \tag{3.12}$$

In equation (3.12), R, γ are the gas constant for the combustion gas which has been calculated using molecular weights of the product elements and using the average values of constant pressure specific heats [6] of the combustion products. The stagnation and exit pressures for nozzles are calculated from the isentropic relations as in equations (3.13) and (3.14) respectively

$$\frac{p_e}{p_0} = (1 + \frac{\gamma-1}{2} {M_e}^2)^{\frac{\gamma}{\gamma-1}} \tag{3.13}$$

$$\frac{\dot{m}_{plasma}\sqrt{T_0}}{A^* p_0} = M^* \sqrt{\frac{\gamma}{R}\left(1 + \frac{\gamma-1}{2} M^*\right)^{\frac{\gamma+1}{\gamma-1}}} \tag{3.14}$$

3.3.3.3 Modelling of MHD generator

The generator in MHD is a segmented Faraday generator. A magnetic field of strength of 2.5 Tesla is applied to the flowing fluid [14]. The conductivity of the fluid is assumed at 10 Seimens/m. The maximum current, maximum voltage, maximum power, and efficiency for the generator are estimated for given magnetic field strength B (Tesla) and electrical conductivity σ (S/m) of working fluid using empirical relations.

The maximum current I_{max} through the generator is obtained using equation (3.15) as

$$I_{max} = \frac{B \times \sigma \times A}{2} \tag{3.15}$$

Maximum voltage developed across the MHD generator v_{max} is given by equation (3.16) as

$$v_{max} = \frac{\mathrm{B} \times V_e \times \mathrm{l}}{2} \tag{3.16}$$

The maximum power density and efficiency can be obtained using equations (3.17), (3.18) respectively.

$$P_{max} = \frac{\sigma \times {V_e}^2 \times B^2}{4} \tag{3.17}$$

$$\eta_{max} = \frac{v_{max}}{V_e x B} \tag{3.18}$$

In equation (3.17), P_{max} is the maximum power, V_e is the nozzle exit velocity, *σ is the assumed electrical conductivity and B* is the magnetic flux. In equation (3.18), η_{max} is the maximum efficiency and v_{max} is the maximum voltage.

3.3.4 Estimation of nozzle exit Mach number

For given area ratios, the nozzle exit Mach number is obtained using the area ratio relation (3.9) above and vice-versa shown in Table 3.2. The nozzle exit gas temperature given by equation (3.10) is the function of two parameters, namely exit Mach number and adiabatic temperature.

Table 3. 2. Computing nozzle exit Mach number

Nozzles	$\frac{A_e}{A^*}$	M_e	γ
A	2.025	2.0	1.104
B	4.126	2.5	1.104

From Table 3.2, it is observed that the nozzle with a smaller area ratio delivers a smaller Mach number at its exit than the one with a higher ratio and vice-versa.

3.3.5. Determination of nozzle parameters at constant nozzle inlet Mach number

It is seen from Table 3.3 that the nozzle exit velocity increases with an increase in exit Mach number but with a corresponding decrease in exit temperature.

Table 3.3. Computation of nozzle parameters

Nozzles	M_i	M_e	$T_0(K)$	$T_e(K)$	$V_e(m/s)$	$\eta_n(\%)$
A	0.7	2.0	3500	2897.35	981.94	99
B	0.7	2.5	3500	2641.50	1096.79	99.9

3.3.6. Calculation of MHD performance parameters

Considering results obtained as shown in Table 3.2 and Table 3.4 and using equations (3.15)-(3.18), it is found that at constant thermal input, the maximum power delivered by the generator increases with an increase in exit velocity or exit Mach number and maximum voltage.

Table 3. 4. Determination of MHD system parameters

Nozzles	Maximum Power (MW/m^3)	Maximum Current (*Amp.*)	Maximum Voltage (*Volt*)	Plant Efficiency (*%*)
A	13.195	12.5	1148.675	50
B	18.598	12.5	1363.75	50

From the estimated data in Table 3.4, it is observed that for the same thermal input, the maximum power density and a maximum voltage obtained from the MHD generator differ for the two nozzles A and B at constant maximum current. The maximum power density and voltage obtainable using a nozzle with a higher area ratio (nozzle B, in this case) is higher.

3.4 Performance analysis of the coal-fired open cycle MHD plant at constant subsonic inlet nozzle Mach number with variation in nozzle area ratio

The present study evaluates the performance of the coal-fired MHD plant operated in an open cycle. The plant is analyzed under the conditions of constant subsonic inlet Mach number while the area ratio of the nozzle is varied. Also, the effects of the variation in nozzle exit Mach number on other parameters are discussed in the following:

3.4.1. Effect of nozzle area ratio on nozzle exit Mach number

Referring to Table 3.2, it has been observed that at a constant specific heat ratio, the nozzle exit Mach number increases with an increase in nozzle exit to throat area ratio. The increase in nozzle exit Mach number is about 25% when the area ratio is increased more than twice its initial value. The change in the Mach number at the nozzle exit due to changes in the nozzle area ratio is shown in Fig. 3.2.

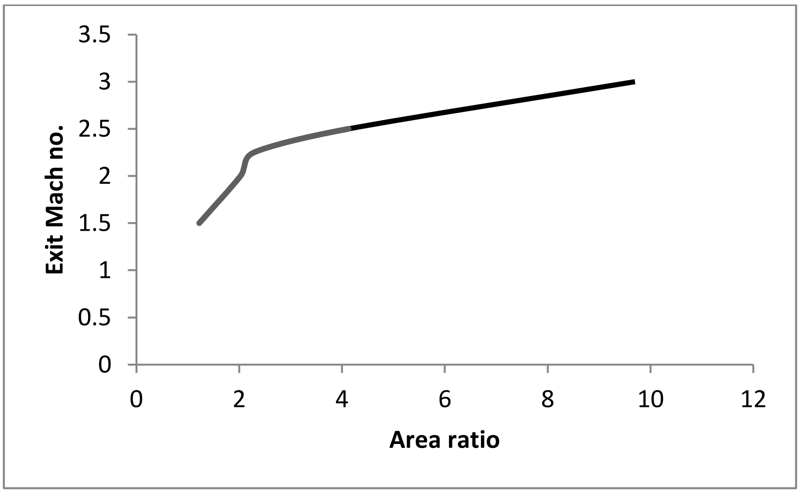

Fig. 3.2. Variation in nozzle exit flow Mach number with area ratio.

3.4.2. Effect of nozzle exit Mach number and adiabatic flame temperature on nozzle exit temperature

The increase in nozzle exit-flow Mach number is due to the influence of the increasing area ratio of the nozzle. At a constant adiabatic flame temperature of 3500 K, there is a decrease in nozzle exit temperature when the nozzle exit Mach number increases, as is shown in Fig. 3.3.

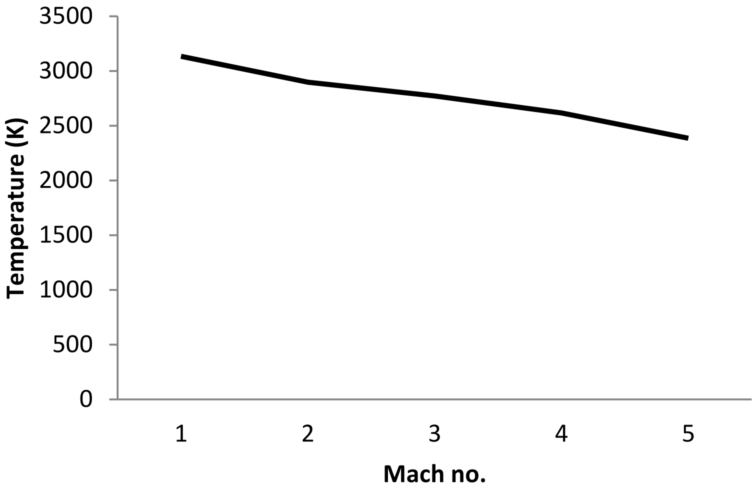

Fig. 3.3. Variation in nozzle exit temperature in *K* with change in exit Mach no.

3.4.3. Effect of nozzle exit Mach number and adiabatic flame temperature on nozzle exit gas velocity

The velocity of the gases at the nozzle exit indicated an increasing trend with the increase in flow Mach number at constant adiabatic flame temperature and constant specific heat ratio. In these situations, the effect of increasing flow Mach number is more pronounced nullifying the effects of decreasing temperature at the nozzle exit. The influence of changing Mach number on the exit velocity in the nozzle is shown in Fig. 3.4.

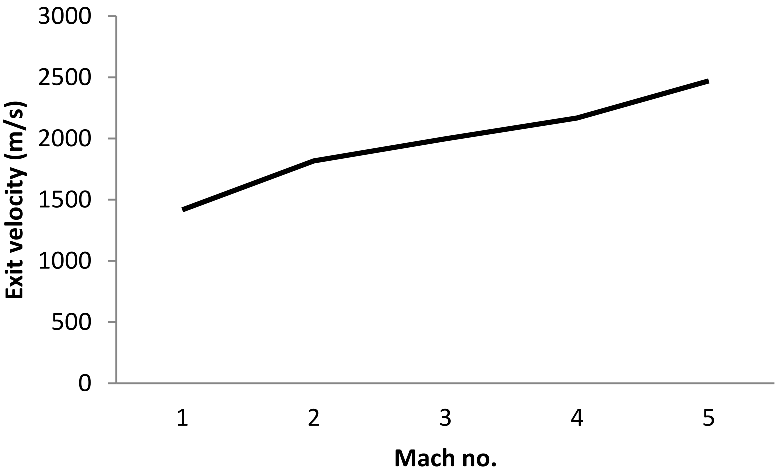

Fig. 3. 4. Variation in nozzle exit gas velocity with Mach no.

3.4.4. Effect of nozzle area ratio on generator maximum power density

At a given gas conductivity and magnetic field strength, an increase in the nozzle area ratio affects the maximum power density in the MHD plant, as shown in Fig. 3.5. The flow Mach number tends to increase with the increase in the area ratio of the nozzle, thereby increasing the gas flow velocity. The relation between gas flow velocity and the power density is given by equation (3.17).

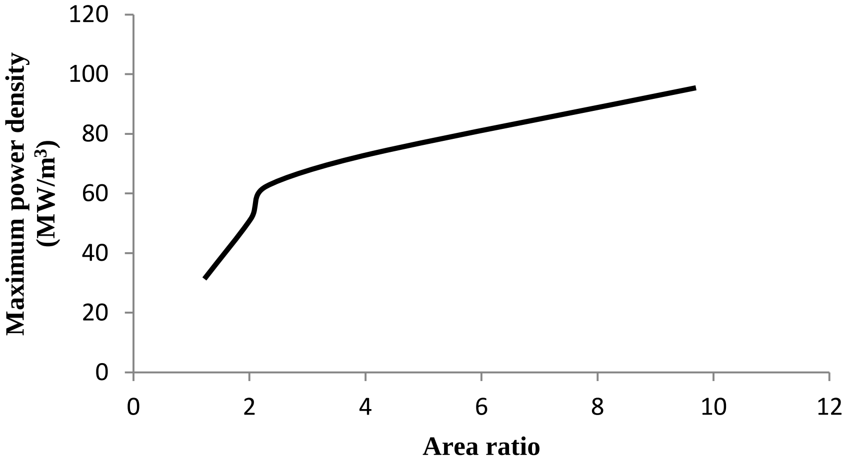

Fig.3.5. Variation in maximum power density with nozzle area ratio.

3.4.5. Effect of generator inlet flow Mach number on maximum voltage at constant thermal input and inlet Mach number

The maximum voltage at the generator of MHD tends to increase with an increase in the flow Mach number at the nozzle exit or generator inlet. As the flow Mach number increases, the gas velocity at the nozzle exit or at the inlet to the MHD generator also increases. As the gas flow velocity at the generator inlet is proportional to the maximum voltage, it leads to an increase in the generator maximum voltage. In this case the inlet Mach number and the thermal input were held constant. The variation is shown in Fig. 3.6.

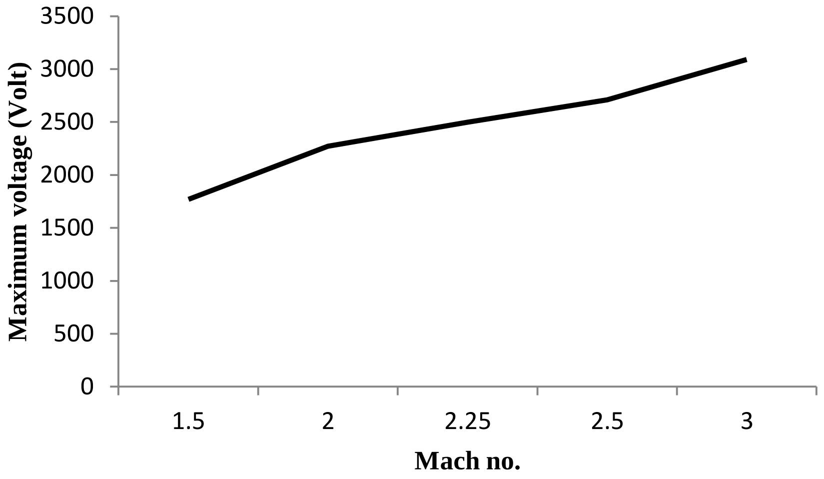

Fig. 3. 6. Variation in maximum voltage with Mach no.

3.4.6. Effect of nozzle area ratio on plant efficiency

For the present MHD plant with the assumed electrical conductivity and magnetic field, any variation in either flow Mach number, gas velocity or the nozzle exit area ratio does not affect the plant maximum efficiency. When the efficiency is evaluated at given applied magnetic field, any change in the nozzle area ratio at its exit section leads to a variation in the generator inlet gas velocity, variation in the flow Mach number and the maximum voltage in a similar proportion. Thus, the MHD plant efficiency is primarily observed to be dependent on the applied magnetic field.

3.5 Summary

In this study, a coal-fired MHD power plant is investigated thermodynamically which operates in an open-cycle mode. The performance of the MHD power plant is analyzed using different area –ratios for the nozzle exit section. The effects of the changes in area ratio on the various parameters that may influence the MHD performance were evaluated.

The variation in area ratio for the nozzle was found to affect the generator inlet temperature which is an important parameter to retain plasma state within the generator volume. The generator inlet flow Mach number, gas velocity, maximum power density, maximum voltage etc. were found to increase as the exit section area ratio for nozzle increases. In the present evaluation the magnetic field strength as well as the gas conductivity were assumed to be constant. The flow Mach number variation within the generator duct resulted in the variation in maximum voltage and power density. It has been observed that at a constant and subsonic nozzle inlet Mach number, the maximum power density and voltage in MHD generator is a function of area ratio and is independent of the thermal input and current produced. However, the nozzle as well as the plant efficiencies remained almost unaffected when the area-ratio is varied.

Thus, the efficiency of the MHD power plant greatly relied upon the strength of applied magnetic field while the maximum power density depends both on the applied magnetic field and the gas conductivity.

Bibliography

[1] Chernyshaw, V. International co-operation in MHD electrical power generation. *IAEA Bulletin*, 20(1): 45-53, 1978.

[2] Assad, M. El. H. Thermodynamic analysis of MHD power cycle. *Journal of Robotics and Mechanical Engineering Research*, 1(1): 7-10, 2015. DOI:10.24218/jrmer.2015.02

[3] Krishnan, R. A. and Jinshah, B. S. Magnetohydrodynamic power generation. *International Journal of Scientific and Research Publications,* 3(6): 1-11, 2013.

[4] Dhareppagol, V.D. and Saurav, A. The future power generation with MHD Generators-Magneto Hydro Dynamic Generation. *International Journal of Advanced Electrical and Electronics Engineering*, 2 (6): 101-105, 2013.

[5] Bejan, A., Tsatsaronis, G., and Moran, M. *Thermal Design and Optimization*. John Wiley & Sons Inc., New York, 1996.

[6] Turns, S. R. *An Introduction to Combustion Concepts and Applications*. McGraw Hill Education Private Limited, India, 3rd edition, 2012.

[7] Channiwala, S. A. and Parikh, P. P. A unified correlation for estimating HHV of solid, liquid and gaseous fuels. *Fuel,* 81: 1051-1063, 2002.

[8] Poonthamil, R., Prakash, S., and Kumar, V. S. A. Enhancement of power

generation in thermal power plant using MHD system. *IOSR Journal of Mechanical and Civil Engineering*, 13: 142-146, 2016.

[9] Ayeleso, A. O. and Kahn, Md. T. E. Modelling of a combustible ionised gas in thermal power plants using MHD conversion system in South Africa. *Journal of King Saud University–Science*, 30: 367-374, 2018.

[10] Cicconardi, S. P. and Perna, A. Performance analysis of integrated systems based on MHD generators. *Energy Procedia*, 45: 1305-1314, 2014.

[11] Sahin, B., Ali, K., and Hasbi, Y. A performance analysis for MHD power cycles operating at maximum power density. *Journal of Physics, D: Applied Physics*, 29: 1473–1475, 1999.

[12] Aithal, S.M. Characteristics of optimum power extraction in a MHD generator with subsonic and supersonic inlets. *Energy Conversion and Management*, 50: 765-771, 2009.

[13] Ibberson, V. J. and Harris, D. Temperature and velocity modulated M.H.D. systems. *Philosophical Transactions of the Royal Society of London, Series A*, 261: 429-439, 1967.

[14] Ambasankaran, C. Status report on the Indian MHD programme. Technical Report No. IN7900136, Indian MHD power generation project, Bhabha Atomic Research Centre Bombay, India, 1978.